Software Simulation and Emulation of Automotive Proton Exchange Membrane Fuel Cell System

D. Rezzak and N. Boudjerda
University of Jijel, LAMEL Laboratory
Jijel, Algeria
d-rezzak@hotmail fr, n_boudjerda@yahoo fr

F. Khoucha
Polytechnic Military Academy of Algiers,
Algiers, Algeria
fkhoucha04@yahoo.fr

Abstract—**Fuel cell power generation technology is gaining importance on its own way as it has many advantages like less environmental pollution, high efficiency, cleanliness and safe operation with the present global scenario of electricity generation, distribution and meeting the consumer demand. Several research works have been done in this area of power generation. In this paper, a dynamic model of a Proton Exchange Membrane (PEM) Fuel Cell (FC) has been developed and the dynamic behavior is studied. PEMFC has been chosen due to its low operating temperature and little start-up time that are suitable for stationary applications like residential and transportation uses. This model is used to simulate and emulate dynamic behavior of FC System (FCS) by using a DC–DC converter, the FC Emulator (FCE) must be able to reproduce the nonlinear output voltage – current (V-I) characteristic of a real FC considering auxiliaries devices.**

Keywords-Fuel cell; dynamic modeling, emulator, power converter

I. INTRODUCTION

Fuel cell stack systems are under intensive development for mobile and stationary power applications [1]. In particular, Proton Exchange Membrane (PEM) Fuel Cells (also known as Polymer Electrolyte Membrane Fuel Cells) are currently in a relatively more mature stage for automotive applications [1].

The fuel cell is an open reactor where hydrogen (or reformed gas) and oxygen (or air) are fed at the inlet of the fuel cell stack depending on the electrical needs, and the by-product is evacuated at the outlet of the stack. The heat generated from the entropy variation during the electro-chemical reaction and the associated irreversible heat sources is also evacuated by a cooling system. In some conditions, the inlet gas should be heated and/or humidified before entering the stack, which requires recovery of water and heat from the outlet of the fuel cell stack. All these requirements are achieved by devices called fuel cell auxiliaries. These auxiliaries are one of the power factors for the efficiency and the durability of a fuel cell system [2]. The auxiliaries design and the control strategies should be adapted to the fuel cell stack operation characteristics and, also validated by tests performed with the fuel cell stack [2].

Even though, there are important needs of a real fuel cell stack for fuel cell system auxiliaries performance tests and validations, the utilization of a fuel cell stack in such a system validation process still impose some drawbacks: the cost of the tests are expensive (e.g., hydrogen consumption), the lifetime of a fuel cell stack is still limited, the fuel cell stack can be damaged during the tests if the auxiliaries are not well designed, and so on [2]. A possible way to reproduce the behavior of a renewable source, whose electrical characteristic (V-I) is nonlinear (as in the case of a Fuel Cell), is to use a DC/DC converter to provide a realistic V-I output characteristic and electrical transient dynamics. All these considerations suggest that any renewable source should be replaced by a hardware system capable of copying its behavior accurately. This hardware system is called emulator. The advantages of using a fuel cell stack emulator to test auxiliaries are obvious: the emulated fuel cell stack power can be configured to different values using the same emulator, depending on the specified fuel cell stack to be emulated; the limit operating scenarios, such as stack short circuits, stack overheats, can be emulated during the tests without damaging a real fuel cell stack [2], [3].

In this paper we are interested to the simulation and the emulation a PEM Fuel Cell (PEMFC). First, we present a model of the fuel cell system taking into account the auxiliary components such as compressor, humidifier, valve, supply and return manifolds. Based on this model, a simulation of the PEMFC shows that the oxygen excess ratio needs a regulation at an optimal value. This has been performed by means of a simple Proportional-Integral (PI) controller. After, the entire model of the FC system including the FC stack and its auxiliaries, as well as the control system of the dc–dc converter, has been implemented on the DSP320F2812 board in the laboratory and the results compared to the simulations. Finally we give a conclusion in which the results and further works are discussed.

II. FUEL CELL MODEL SYSTEM

The fuel cell system used in this study is based on the control oriented model explained in [4],[5] which is developed based on physical mass and energy conservations along with electrochemical, thermodynamic and fluid flow principles. A simplified scheme of the system is given in Fig.1.

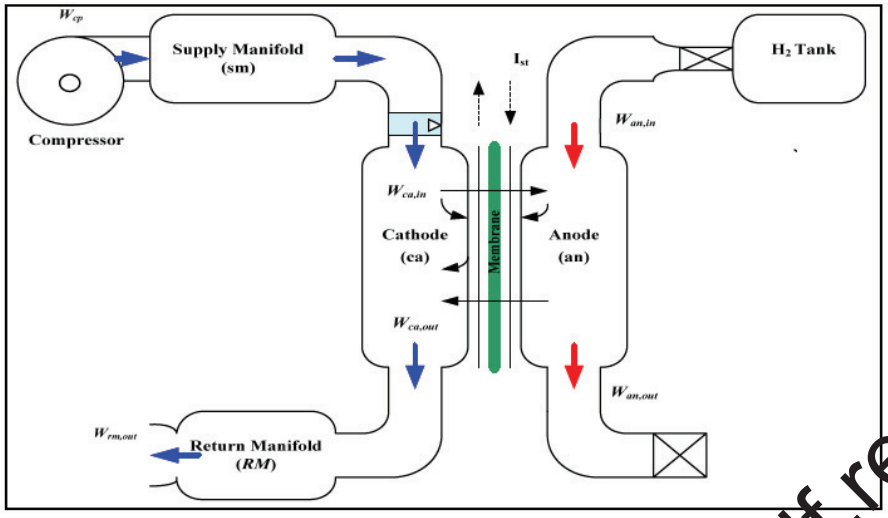

Figure 1. Simplified scheme of the fuel cell system

The model represents a system with 75 kW PEM fuel cell stack composed of 381 cells with a current capability of 310 A. The fuel cell stack represented by anode and cathode flow, membrane hydration and polarization curve models, is augmented with the model of auxiliary components including: compressor, humidifier, valve, supply and return manifolds. Two main assumptions are used in the FCS simulation [4], [5]. First, the stack humidity and temperature are considered perfectly regulated to the desired levels and thus the effect of temperature and humidity fluctuations are not considered. This assumption follows the fact that the humidity and temperature dynamics are much slower than FCS flow and power dynamics. Second, the fuel supply is considered instantaneous and provided by pure hydrogen. The hydrogen flow control is assumed to always be able to regulate the pressure difference across the membrane to prevent membrane damage. With these assumptions, the control problem is limited to the subsystem of air management [4], [5].

A. *Cathode Flowsystem*

The complete equations and explanations can be found in [5]. The compressor supplies the air flow following the command to its motor. The supply manifold, cathode channels and return manifold all act as a gas storage volume. The end of the return manifold connects to atmosphere through an actuator valve. The compressor dynamics related to its inertia

$$J_{cp}\frac{d\omega_{cp}}{dt} = \left(\tau_{cm} - \tau_{cp}\right) \tag{1}$$

Where J_{cp} (kg.m2) is the compressor inertia, ω_{cp} (rad/s) is the compressor speed; τ_{cm} (N m) and τ_{cp} (N m) are compressor motor torque and compressor load torque, respectively. The compressor speed computed by integrating Eq. (1), and the downstream pressure, i.e. supply manifold pressure, p_{sm} (atm), influence different air flow rates through the compressor, W_{cp} (kg/s).

The compressor air flow flows into the supply manifold thus influence the changes in the pressure inside the supply manifold through mass and energy conservation laws

$$\frac{dm_{sm}}{dt} = w_{cp} - w_{sm,out} \tag{2}$$

$$\frac{dp_{sm}}{dt} = \frac{\gamma R_a}{V_{sm}}\left(W_{cp}T_{cp,out} - W_{sm,out}T_{sm}\right) \tag{3}$$

Where m_{sm} (kg) is the air mass in the supply manifold and $W_{sm,out}$(kg/s) is the air flow out of the supply manifold into the stack cathode volume which is a function of the supply manifold pressure. V_{sm} (m3) is the supply manifold volume, R_a (N.m/K) is the gas constant of air and γ is the ratio of the specific heat capacities, which in case of air is 1.4 [5]. $T_{cp,out}(K)$ and T_{sm} (K) are the temperature of the air at compressor outlet and that of the air inside the supply manifold respectively.

The change in supply manifold pressure affects the rate of air entering the stack cathode through the linear nozzle Eq. (4), where $k_{sm,out}$(kg.atm/s) is the supply manifold nozzle constant

$$W_{sm,out} = k_{sm,out}\left(p_{sm} - p_{ca}\right) \tag{4}$$

The air flow rate into the cathode ($W_{sm,out}$) then affects the oxygen level in the cathode, and therefore affects the stack voltage and the stack power output. The dynamic of the oxygen level in the cathode is governed by the mass conservation law. There are three states in the cathode volume model, namely the oxygen mass $m_{O2,ca}$, the nitrogen mass $m_{N2,ca}$ and the vapor mass $m_{w,ca}$; their state equations are

$$\begin{cases} \dfrac{dm_{O2,ca}}{dt} = W_{O2,ca,in} - W_{O2,ca,out} - W_{O2,ca,reacted} \\ \dfrac{dm_{N2,ca}}{dt} = W_{N2,ca,in} - W_{N2,ca,out} \\ \dfrac{dm_{w,ca}}{dt} = W_{v,ca,in} - W_{v,ca,out} - W_{v,ca,reacted} \end{cases} \quad (5)$$

Where, $W_{O2,ca,in}$ (kg/s) and $W_{O2,ca,out}$ (kg/s) are the mass flow rates of oxygen gas entering and leaving the cathode, $W_{N2,ca,in}$ (kg/s) and $W_{N2,ca,out}$ (kg/s) are the mass flow rates of nitrogen gas entering and leaving the cathode, $W_{v,ca,in}$ (kg/s) and $W_{v,ca,out}$ (kg/s) are the mass flow rates of vapor entering and leaving the cathode, $W_{v,ca,gen}$ (kg/s) is rate of vapor generated in the fuel cell reaction, $W_{l,ca,out}$ (kg/s) is rate of liquid water leaving the cathode and $W_{v,membr}$ (kg/s) is flow rate of water transfer across the membrane. The oxygen partial pressure which affects the stack voltage can be calculated from these states using the ideal gas law. The mass flow rates with subscript 'in' are calculated from $W_{sm,out}$ and the air thermodynamic properties. The amount of oxygen reacted or used in the reaction, $W_{O2,react}$ (kg/s), is a function of stack current, I_{fc} (A), which is considered in this work as a disturbance input

$$W_{O2,react} = M_{O2}\frac{nIfc}{4F} \quad (6)$$

Where n is the number of cells of the stack, M_{O2} is the molar mass of oxygen (kg/mol) and F is the Faraday's number (C/mol). The mass flows with subscript 'out' are functions of the states ($m_{O2,ca}$, $m_{N2,ca}$ and $m_{w,ca}$) and the cathode outlet flow, which is a function of the pressure downstream, i.e. return manifold pressure, p_{rm} (atm). The function in the linear nozzle Eq. (7) is in the same form as Eq. (4), where $k_{ca,out}$(kg.atm/s) is the return manifold nozzle constant and p_{ca} (atm) is the pressure of the cathode

$$W_{ca,out} = k_{ca,out}\left(p_{ca} - p_{rm}\right) \quad (7)$$

The dynamic of the return manifold pressure is

$$\frac{dp_{rm}}{dt} = \frac{R_a T_{rm}}{V_{sm}}\left(W_{ca,out} - W_{rm,out}\right) \quad (8)$$

Where T_{rm} (K) is the temperature of the gas in the return manifold and V_{rm} (m3) is the return manifold volume. The return manifold outlet flow, $W_{rm,out}$ (kg/s), is calculated by a nonlinear nozzle equation.

B. Anode Flow Model

Similar to the cathode flow model, we determine hydrogen partial pressure and anode flow humidity by balancing the mass flow of hydrogen $m_{H2,an}$, and water $m_{w,an}$ in the anode

$$\begin{cases} \dfrac{dm_{H2,an}}{dt} = W_{H2,an,in} - W_{H2,an,out} - W_{H2,ca,reacted} \\ \dfrac{dm_{w,an}}{dt} = W_{v,an,in} - W_{v,an,out} - W_{v,membr} \end{cases} \quad (9)$$

In this model, it is assumed that pure hydrogen gas is supplied to the anode by the hydrogen tank and the anode inlet flow rate is instantaneously adjusted by a valve to maintain minimum pressure difference across the membrane. This can be achieved by using a high gain proportional controller of hydrogen flow rate such that the anode pressure p_{an} tracks the cathode pressure p_{ca}. The inlet hydrogen flow is assumed to have 100% relative humidity. The anode outlet flow represents the hydrogen purge and is currently assumed to be zero. The temperature of the flow is assumed to be equal to the stack temperature. The rate of hydrogen consumed in the reaction, $W_{H2,reacted}$, is a function of both of the stack current I_{st} and the hydrogen molar mass M_{H2} [4]-[6]

$$W_{H2,reacted} = M_{H2}\frac{NI_{st}}{2F} \quad (10)$$

C. Membrane Hydration Model

The mass flow of vapor across the membrane $W_{v,membr}$ is calculated using mass transport principles and membrane properties given in [4] according to

$$W_{v,membr} = M_v A_{fc}\left(\frac{n_d}{\rho_m}\frac{i}{F} - D_w\frac{\left(\phi_{v,ca} - \phi_{v,an}\right)}{t_m}\right) \quad (11)$$

A_{fc} is the active area of the FC, i is the FC current density (current per active area, I_{st}/A_{fc}) and t_m is membrane thickness. The electro-osmotic coefficient n_d is function of $\phi_{v,ca}$ and $\phi_{v,an}$. The diffusion coefficient D_w is function of $\phi_{v,ca}$, $\phi_{v,an}$ and T_{st}.

D. Fuel cell voltage

Proton exchange membrane fuel cells (PEMFC) combine hydrogen and oxygen over a platinum catalyst to produce electrochemical energy with water as the byproduct. Figure 2 shows the (v_{fc}-i) characteristic of a typical single cell operating at *Tfc=80 °C* and different air pressure [5], [6]. The variation of individual cell voltage is found from the maximum cell voltage and the various voltage losses. Multiple factors contribute to the irreversible losses (voltage drop) in real fuel cell that cause the cell voltage to be less than its ideal potential [5]-[7]. The losses, which are also called polarization, irreversibility, or over voltage, over potential, originate primarily from three sources: a) activation polarization, b) ohmic polarization, and c) concentration (mass transport) polarization. Each of these is associated with a voltage drop and they are dominant in different regions of current density. Figure 2 shows the different regions and the corresponding polarization effects. The ideal voltage is the maximum voltage that each cell in the stack can produce at a given temperature with the partial pressure of the reactants and products known. The output voltage of a single cell v_{fc} can be given by [5]-[8]

$$v_{fc} = E - v_{act} - v_{ohm} - v_{conc} \quad (12)$$

Where E is the thermodynamic potential of the cell, it represents the no-load reversible voltage, v_{act} is the activation overpotential, v_{ohm} is the ohmic overpotential and v_{conc} is the concentration overpotential.

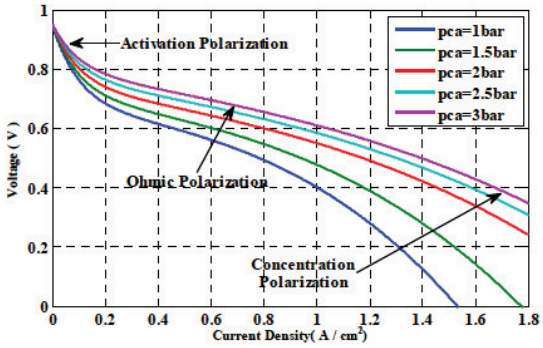

Figure 2. Fuel cell polarization curve fitting results at 80 C

A higher voltage is obtained by connecting n cells in series

$$v_{st} = n v_{fc} \tag{13}$$

1) Cell reversible voltage: The reversible voltage E is computed from a modified version of Nernst equations, considering the variations of temperature from the standard value of 25 °C.

$$E = 1.229 - 0.85\times10^{-3}\left(T_{fc} - 298.15\right) + 4.3085\times 10^{-5} T_{fc}\left[\ln(p_{H2}) + \frac{1}{2}\ln(p_{O2})\right] \tag{14}$$

T_{fc} is the fuel cell temperature in (K), p_{H2} and p_{O2} are the hydrogen and oxygen partial pressures in (atm) respectively.

2) Activation overpotential: The activation overpotential v_{act} is expressed by [4], [5]

$$v_{act} = v_0 + v_a\left(1 - e^{-c_1 i}\right) \tag{15}$$

Where, v_0 (V) is the voltage drop at zero current density. The values of the constant parameters v_a (V), c_1 and their dependency on the oxygen partial pressure and temperature can be determined from a nonlinear regression of experimental data using the basis function in Eq. (15).

3) Ohmic voltage drop: The ohmic voltage drop (v_{ohm}) is caused by the electrons transfer through the collecting plates and the carbon electrodes and by the protons transfer through the solid membrane. It is expressed by

$$v_{ohm} = R_{ohm} i \tag{16}$$

Where, R_{ohm} ($\Omega.cm^2$) is the internal resistance. It depends strongly on the membrane humidity and the cell temperature [5], [6]. It can be written as a function of the membrane thickness t_m and conductivity σ_m $(\Omega.cm)^{-1}$ as follows

$$R_{ohm} = \frac{t_m}{\sigma_m} \tag{17}$$

The conductivity σ_m is a function of the membrane water content λ_m and fuel cell temperature. For λ_m between 0 and 14 corresponds to the relative humidity between 0% and 100% [5]. Its variation with humidity and temperature is [5]-[7]

$$\sigma_m = (b_{11}\lambda_m - b_{11})\exp\left(b_2\left(\frac{1}{303} - \frac{1}{T_{fc}}\right)\right) \tag{18}$$

The coefficients b_{11}, b_{12} and b_2 are usually determined empirically [5]-[7].

4) Concentration overpotential: To define this voltage drop term, a maximum current density i_{max} is defined, with which the cell works at the same rate of the maximum supply speed. On this basis, the concentration overpotential (v_{conc}) can be expressed by

$$v_{conc} = i\left(c_2 \frac{i}{i_{max}}\right)^{c_3} \tag{19}$$

Where c_1, c_3 and i_{max} are constants depending on the temperature and the reactant partial pressure and can determined empirically. The parameter i_{max} is the current density that causes precipitous voltage drop.

E. Air management control

The controlled variable is the oxygen excess ratio λ_{O2}

$$\lambda_{O2} = \frac{W_{O2,in}}{W_{O2,react}} \tag{20}$$

Where $W_{O2,in}$ is the supplied oxygen and $W_{O2,react}$ is the oxygen consumed in the reaction. A low value of λ_{O2} means excessive depletion of oxygen in the cathode (oxygen starvation) which results in the decrease of the stack voltage and delivered power as well as shortening the life of the FC stack. For simplicity reasons $\lambda_{O2} = 2$ is considered as an optimal set-up value [4]-[6]. The main goal of the air management control is to keep the output at the level ($\lambda_{O2} = 2$), regardless of the current demanded by the load, which is considered as an input disturbance. The input variable of the FC system is the compressor motor voltage v_{cm}. This can be done by using various types of controllers [4], [5]; in this work we propose the use of simply a Proportional-Integral (*PI*) controller.

III. Simulation Of The FCS With Regulated λ_{O2}

The air management has to comply with the requirement that $\lambda_{O2} = 2$. For this purpose, a constant ($\lambda^*_{O2} = 2$) is given to the system as a reference variable, a simple solution is the use of a *PI* controller of the air flow rate, which would guarantee zero steady-state error of the system as well as its stability. For calculating the parameters of PI controller, the nonlinear model of the simplified system needs to be linearized [4].

Figure 4 shows the implemented control scheme of λ_{O2}. The output v_{cm} of the *PI* controller is the reference voltage of the compressor motor. It should be remarked that the coefficient λ_{O2} is not a measured variable, but is inferred by the nonlinear model of the FC system, which would then act as an observer of the real value. In our application it is assumed that the fed-back λ_{O2} coincides with the real value.

Figure 5 shows the simulation results of the FCS model. For a variable input disturbance i_{st} (Fig. 4.a) we see clearly that λ_{O2} is regulated at the reference value (λ^*_{O2}=2), (Fig. 4.b). However, this is accompanied with a variation of the output voltage (Fig. 4.d) which needs to be regulated for automotive applications where a DC-DC or DC-AC converter is generally connected which allows regulating directly the output voltage of the converter. We see also (Fig. 4.c) that the transient behavior of the regulated λ_{O2} is greater than 2 seconds; thus, its dynamic needs improvement in further works [4].

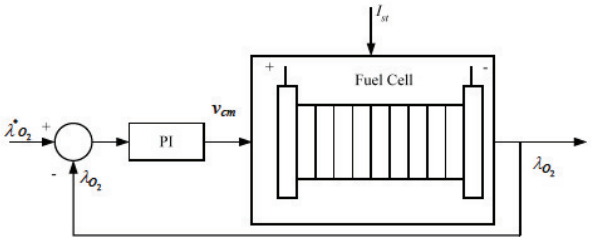

Figure 3. Block diagram of the PI λ_{O2} control scheme

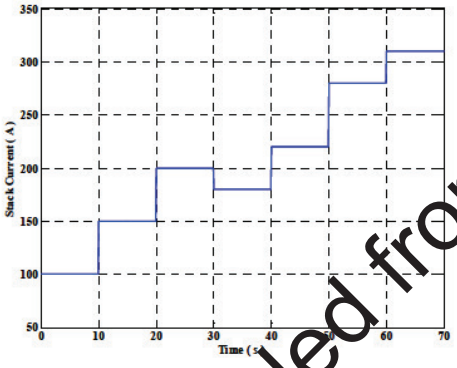

(a). Stack current

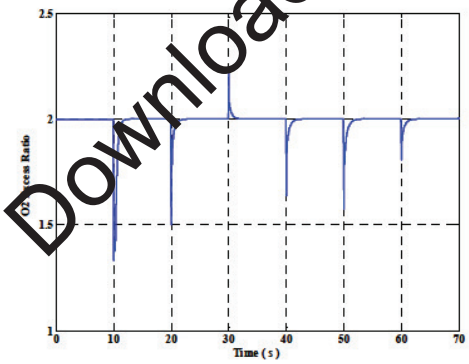

(b). Oxygen excess ratio λ_{O2}

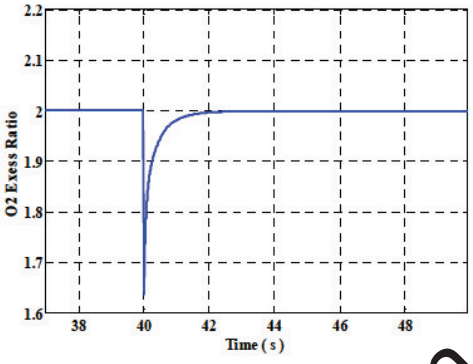

(c). Zoom of Oxygen excess ratio λ_{O2}

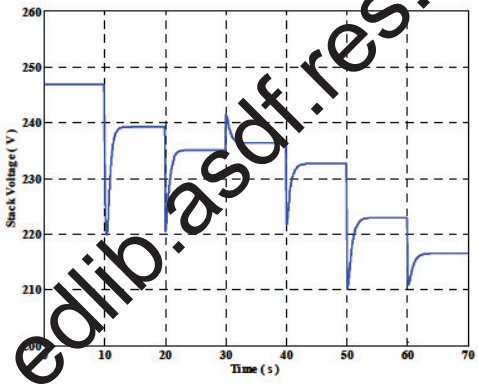

(d). Stack voltage v_{st}

Figure 4.Simulation results of the fuel cell system model for a series of input step change.

IV. FUEL CELL EMULATOR

In this section an equivalent block diagram of the FC system emulator is implemented in the laboratory and experiments have been carried out. According to the bloc diagram of Fig. 5 the main elements are the dynamic model block of the FC system described previously: The inputs of the model are: the stack temperature T, the electric current required by the load I_{FC} and pressions (p_{ca}, p_{O2} and p_{H2}). We notice that the stack temperature T is assumed to be constant (T = 80 °C). The controller output is v_{ref} the reference value of the stack voltage. The first part of this system gives the output voltage of the PEM according to the parameters characterizing the operating conditions of fuel cell system (temperature, pressure, etc). The reference voltage V_{fcref} is obtained by a software implementation in the DSP board. The second part is formed by a hardware full bridge DC-DC converter. The resulting PWM switching signals δ (Fig. 5) allows the output voltage of the converter to track the model fuel cell voltage reference [3].

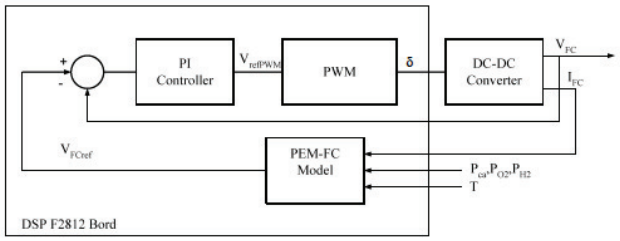

Figure 5. Block diagram

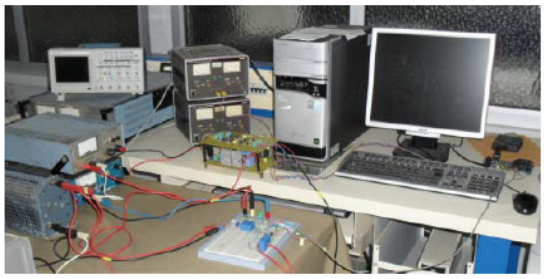

Figure 6. Experimental setup

V. EXPERIMENTAL RESULTS

A prototype of the FC emulator (Fig. 6) has been built in the laboratory. The dc-dc IBGT full bridge converter has a rated power of 150 W, with DC link voltage V_{DC} = 15 V and a rate current I_{FCE} = 10 A. The system therefore emulates a PEM-FC with 381 cells. In order to make the experimental results consistent with those of the model, the output current of the emulator has been scaled up by the factor 130, so as to have a current ranging from 0 to 700 A, while the output voltage of the emulator has been scaled up by the factor 381/15 so as to have a voltage ranging about from 0 to 500 V.

Experimental results have been performed in *Matlab/Simulink* environment adopting the FCS emulator. The model of the FC system, as well as the control system of the dc–dc converter has been implemented on the DSP320F2812 board. Figure 8 illustrates the stack characteristics at different cathode pressures. It shows that simulations (continuous lines) and the experimental results of the emulator built in this work based on the DC-DC converter (points) are super imposable.

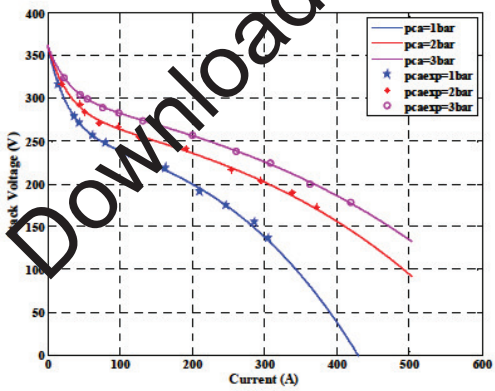

Figure 7. Simulation and emulation results of the stack Fuel cell curve fitting

VI. CONCLUSION

In this paper we are interested to the simulation and the emulation a PEM Fuel Cell (PEMFC). First, we present a model of the fuel cell system taking into account the auxiliary components such as compressor, humidifier, valve, supply and return manifolds. Based on this model, a simulation of the PEMFC shows that the oxygen excess ratio needs a regulation at an optimal value. This has been performed by means of a simple Proportional-Integral (PI) controller. After, the model of the FC system, as well as the control system of the dc–dc converter has been implemented on the DSP320F2812 board in the laboratory and the results compared to the simulations. The DC/DC converter, suitably driven, can accurately describe the current-voltage characteristic of a Fuel Cell.

APPENDIX

PARAMETERS FOR FUEL CELL SYSTEM

$\rho_{m\,dry}$(0.002 Kg/cm^3), $M_{m\,dry}$ (1.1 Kg/mol), t_m (0.01275 cm), n (381 cells), A_{fc}(280 cm^2), J_{cp}(5.10^{-5}$kg.m^2$), v_{an} (0.00[illegible] m^3), v_{cm} (0.02 m^3), v_{rm} (0.005 m^3), $C_{d\,rm}$ (0.0124 m^2), $A_{t\,rm}$ (0.002 [illegible]), $K_{an\,out}$(0.3629.10^{-5}kg/mol), $K_{ca\,out}$(0.2177.10^{-5}kg/mol), k_v(0.0153 [illegible]$/rad\,s^{-1}$), k_t(0.0153 Nm/A), R_{cm} (0.9[illegible]), η_{cm} (98 %)

REFERENCES

[1] Liyan Zhang, Min Pan, Shuhai Quan, Qihong Chen and Ying Shi "Adaptive Neural Control Based on PEMFC Hybrid Modeling" 2006 IEEE. 1-4244-0332-4/06.

[2] FeiGao, Benjamin Blunier, David Bouquain, Abdellatif Miraoui and Abdellah EL Moudni "Polymer Electrolyte Fuel Cell Stack Emulator for Automotive Hardware-In-the-Loop Applications",2009IEEE. 978-1-4244-2601-0/09.

[3] M. Cirrincione, M. C. Di Piazza, G. Marsala, M. Pucci, G. Vitale, "Real Time Simulation of Renewable Sources by Model-Based Control of DC/DC Converters", 2008 IEEE, 978-1-4244-1666-0/08.

[4] G. Marsala, D. Bouquin, J.T. Pukrushpan, M.Pucci, G. Cirrincione, G. Vitale, A. Miraoui. "A Neural Inverse Control of a PEM-FC System by the Generalized Mapping Regressor (GMR)". 2008 IEEE, 978-1-4244-2279-1/08.

[5] Jay T Pukrushpan, HueiPeng, Anna G Stefanopoulou, "Simulation And Analysis Of Transient Fuel Cell System Performance Based On A Dynamic Reactant Flow Model", Proceedings of IMECE'02 2002 ASME International Mechanical Engineering Congress & Exposition November 17-22, 2002, New Orleans, Louisiana, USA.

[6] Jay T. Pukrushpan, Huei Peng, Anna G. Stefanopoulou, «Control-Oriented Modeling and Analysis for Automotive Fuel Cell Systems» Journal of Dynamic Systems, Measurement, and Control, Vol. 126 MARCH 2004.

[7] J.T. Pukrushpan, A.G. Stefanopoulou and H. Peng, «Control of Fuel Cell Breathing,» IEEE Control System Magazines, Vol.24, No.2, pp. 30-46, April 2004.

[8] J. Larminie and A. Dicks, "Fuel Cell Systems Explained", West Sussex, England, John Wiley & Sons Inc, 2000.